Triggering extreme events at the nanoscale in photonic seas

C. Liu[1], R. E. C. van der Wel[2], N. Rotenberg[2], L. Kuipers[2], T. F. Krauss[3], A. Di Falco[4] and A. Fratalocchi[1*]

[1]*PRIMALIGHT, Faculty of Electrical Engineering; Applied Mathematics and Computational Science, King Abdullah University of Science and Technology (KAUST), Thuwal 23955-6900 Saudi Arabia*

[2]*Center for Nanophotonics, FOM Institute AMOLF, Science Park 104, 1098 XG Amsterdam, The Netherlands*

[3]*Department of Physics, University of York, Heslington, York, YO10 5DD, UK*

[4]*School of Physics and Astronomy, University of St. Andrews, North Haugh, St. Andrews KY16 9SS, UK*

(Dated: March 31, 2015)

Abstract

Hurricanes, tsunami, rogue waves and tornadoes are rare natural phenomena that embed an exceptionally large amount of energy, which appears and quickly disappears in a probabilistic fashion. This makes them difficult to predict and hard to generate on demand. Here we demonstrate that we can trigger the onset of rare events akin to rogue waves controllably, while we can systematically use their generation to break the diffraction limit of light propagation. We illustrate this phenomenon in the interesting case of a random field, where energy oscillates among incoherent degrees of freedom. Despite the low energy carried by each wave, we illustrate how to control a mechanism of spontaneous synchronization, which constructively builds up the spectral energy available in the whole bandwidth of the field into giant coherent structures, whose statistics is perfectly predictable. The larger the frequency bandwidth of the random field, the larger the amplitude of rare events that are built up by this mechanism. Our system is composed of an integrated optical resonator, realized on a photonic crystal chip. Trough near field imaging experiments, we record the most confined rogue waves ever reported, characterized by a spatial localization of 206 μm and with ultrashort duration of 163 fs at the wavelength $\lambda = 1.55\ \mu m$. Quite remarkably, such localized energy patterns are formed in a deterministic dielectric structure that does not require nonlinear properties.

* andrea.fratalocchi@kaust.edu.sa; www.primalight.org

INTRODUCTION

The extreme localization of waves, either in space or in time, has always been the subject of great interest in science. Subwavelength manipulation of light has driven a large body of research in metamaterials and plasmonics, where metallic nanostructures and negative index materials have been investigated to achieve energy compression, ultra-high efficient photovoltaics and superlens effects [1–7]. Nanofocusing of light has also stimulated new concepts in subwavelength imaging [8, 9], including the use of disorder with spatial light modulators to trap photons beyond the diffraction limit [10, 11]. The study of electromagnetic confinement on short temporal scales, conversely, is at the frontier of research in ultrafast optics, where ultimately it led to the development of advanced refocusing techniques and single-cycle laser sources [12–14]. Even though this body of research spans across very different areas, they are all characterized by the use of deterministic effects and predictable events, which impose the development of challenging fabrication processes, sophisticated experimental apparatus and/or elaborate wavefront reshaping techniques. On the other hand, extreme localization of energy naturally arises in rare events such as hurricanes, rogue waves, and tsunami, which happen to appear at once and then disappear again. Apart from their catastrophic nature, these phenomena are normally not exploited due to their unpredictability, which makes it difficult to understand their physics and control their emergence. Among various types of rare dynamics, rogue waves are particularly interesting. Rogue Waves (RW) are isolated events in wave motion that are characterized by the appearance of localized waveforms with exceptional amplitude. These events seem ubiquitous and reported in a large number of systems, which share diverse degrees of randomness, noise, unpredictability, linear and nonlinear responses [15–27]. A key issue is the active role of randomness [26, 27], and the question whether RW can be observed in fully deterministic structures with no intrinsic disorder. Deterministic systems are more easily controlled, they can provide a simpler platform for studying the physics of these phenomena, and they can challenge us with an intriguing problem: can we embed the exceptional amount of energy of a rogue wave into a simple integrated structure? And if this structure can be engineered, what are the specific limits we can break with the unique properties of these events? The ubiquitous character of RW manifested in uniform media —such as water— and without relying on any particular geometry, has the potential to open a new paradigm where extreme events are not only in-

vestigated for their elusive physics, but can also be source of inspiration for unconventional light management techniques.

In this Article, we report the ultrafast localization of photons by exploiting a new mechanism for the generation of rogue waves, which also allows to gain new fundamental insights on the properties of these events. Given an ensemble of strongly incoherent waves propagating into a linear material, we here show how is possible to coherently use the spectral energy contained in the whole bandwidth of the field by creating ultrafast subwavelength rare events, whose statistics is generated on demand by controlling the phase probability distribution of the ensemble. When phases are uniformly distributed in $[0, 2\pi]$, in particular, light experiences a classic random walk and rogue waves are not observed. Conversely and contrary to intuition, when a small perturbation is applied and a portion of the phase-space in $[0, 2\pi]$ is not explored, rare events of large intensity settle in. Quite interestingly, these events manifest also in the presence of an extremely small perturbation. The formation of such structures results from a mechanism of spontaneous synchronization, which coherently builds up energy into giant structures.

We design an integrated photonics chip in two dimensional photonic crystal (PhC) where these phenomena can be generated in controlled conditions. Our system is composed by PhC resonator, whose shape has been suitably engineered in a quarter-stadium form. This particular shape has been chosen to allow the generation of the incoherent wave ensemble through the mechanism of wave chaos [28]. Even though the material does not exhibit any nonlinearity, the stadium shape supports chaotic motion for light rays, and fully randomize any input wavefront into an ensemble of strongly incoherent waves. Phase control in the wave ensemble is then achieved by using tunable losses, represented by outgoing waveguide channels of specific widths. Our integrated chips, together with State-of-the-Art Near Field Scanning Optical Microscope (NSOM) imaging techniques [29], allow us to measure both the amplitude and the phase of light with nanometre and femtosecond accuracy. In our integrated platform, we triggered the experimental generation of ultrafast (163-fs long) and subwavelength (206nm wide) rogue waves at the wavelength $\lambda = 1.55\mu$m.

RESULTS

Extreme rare events from spontaneous synchronizations of incoherent waves

We begin our analysis by investigating the generation of localized rare events from an incoherent sea of random waves $\psi(\mathbf{r}, t)$, which can be decomposed in Fourier domain as follows:

$$\psi(\mathbf{r}, t) = \int a(\mathbf{k}, \omega) \cdot e^{i(\omega t - \mathbf{k}\cdot\mathbf{r} + \phi(\mathbf{k},\omega))} d\omega d\mathbf{k}, \tag{1}$$

with $a(\mathbf{k}, \omega)$ and $\phi(\mathbf{k}, \omega)$ random amplitudes and phases, respectively, depending on the wavevector $\mathbf{k}$ and frequency ω. If a and ϕ are distributed uniformly, Eq. (1) describes a classical random walk whose intensity probability density $P(I) = P(|\psi|^2)$ follows a Rayleigh law $P(I) = \exp(-I)$, as confirmed in Fig. 1a. This case was simulated with an ensemble of 2000 random waves with amplitudes $a(\mathbf{k})$ uniformly distributed in $[0, 1]$, with randomly displaced wavevectors $|\mathbf{k}| < 2\pi/\lambda$ and uniformly distributed frequencies $\omega \in [1, 2]$. For these conditions, no rare event of large intensity is generated (Fig. 1b). If we apply a suitably small perturbation to the system, however, we observe a radically different scenario. Figures 1c-d illustrate what happens when the phase probability distribution gets *diluted* by, e.g., a range of inaccessible values for ϕ (Fig. 1c inset). We observe an anomalous deviation from the Rayleigh law and the appearance of a rare event (Fig. 1c circle markers). The deviation from the Rayleigh law shown in Fig. 1c has the characteristic "L" shape with a long tail, which is the hallmark for the appearance of rogue waves (Fig. 1d). Considering the small magnitude of the perturbation $\delta\phi = \pi/10$, the generation of rare events of strong amplitude ($\approx 60\%$ higher than the Rayleigh limit) is quite remarkable.

The generation of rare events deviating from the Rayleigh law can be intuitively explained by using the concept of path cancellation, which is usually developed to study the dynamics of random walks subjected to different physical constraints [30]. This approach is in general very involved, and its detailed analysis is deferred to a future work, while we here summarize the main physical results. In a classical random walk of light with no dilution, the intensity is Raleigh distributed and, after n steps, the point of maximum intensity I_n is observed with the lowest probability density $P(I_n) = e^{-I_n}$. The value I_n can be obtained by different combinations of waves with random amplitudes and phases; however, there exists at least a situation where I_n is generated after n steps in the following configuration: a set of waves

that destructively interfere and whose phase is randomly distributed in a region of width δ, and all the remaining waves that constructively interfere in all possible angular directions. This event is, by definition, rare and observed in one (or very few) spatial point, which we label p. When we dilute the random walk and make the gap δ inaccessible, the resulting field evolution shows the same paths of the case with no dilution, minus all the paths originated by the waves whose phase lies in the gap δ. The removal of these paths now enable in p the appearance of a rare event where all the waves constructively interfere, or equivalently, get synchronized. The intensity generated in p is now larger than the Rayleigh limit I_n, due to the removal of the components that were interfering destructively. Such a rare event can be expressed as follows:

$$\Psi(\mathbf{r},t) = \int a_0 \cdot \exp[i(\omega t - \mathbf{k}\cdot\mathbf{r} + \phi_0)] d\omega d\mathbf{k}, \tag{2}$$

with ϕ_0 a generic constant value. Equation (2) can be regarded as a spontaneous synchronization of statistical origin. When such a synchronization involves all spectral frequencies ω of the field, the resulting intensity reaches the largest possible value for that particular field and the spectral energy contained in the whole frequency bandwidth of the system is coherently summed up. Notably, Eq. (2) embeds a super-oscillatory [31] nature that beats the diffraction limit even when only diffraction limited components are allowed to interfere. In particular, if we consider a buildup process where all the possible components $k = |\mathbf{k}| < 2\pi/\lambda$ are summed up, by integrating (2) we obtain:

$$\Psi(\mathbf{r},t) \propto J_0(k\cdot|\mathbf{r}|)\frac{\sin\left(\frac{\delta\omega}{2}t\right)}{t}, \tag{3}$$

with $\delta\omega$ the frequency bandwidth where Eq. (2) holds. Equation (3), in intensity, exhibits a subwavelength spatial Full Width Half Maximum (FWHM) that is 25% smaller than the diffraction limit $\lambda/2$, and a time FWHM of $\tau = 2\pi/\delta\omega$. Subwavelength confinement originates from the Bessel wave $J_0(k\cdot r)$, which is able to oscillate faster that its band limited Fourier components due to super-oscillations. Super-oscillations are largely investigated for the realization of superlenses [8], although super-resolution usually comes at the expense of side lobes that can be several orders of magnitude higher than the subwavelength spot. The rogue wave nature of our rare event, conversely, always guarantees that super oscillatory behaviors are observed as bright energy spots with small sidelobes, offering a natural pathway to overcoming this problem. The brightness of the coherent energy spot depends on the

spectral bandwidth $\delta\omega$ of the waves that get synchronized: the larger the bandwidth, the larger the energy peak of the rogue wave.

In order to illustrate the generation of ultrafast, sub-λ rogue waves in an integrated structure, we design two dimensional PhC optical cavities with losses controlled by the width of the output channels (Fig. 2a). Light of a frequency within the bandgap of the photonic crystal can escape from the system only via the input/output channels, while getting reflected at the resonator boundaries. Wave chaos [28] fully randomizes light reflections at the resonator boundaries and generates a "photonic sea" of incoherent waves, where diffraction-limited contributions are continuously mixed up. In this dynamics, light rays can only escape into the output channels.

In order to provide an intuitive physical explanation of the consequences of the removal of a set of light rays from the dynamics of the system, we used the same idea of path cancellation previously introduced to analyze the formation of rare events. When outgoing channels are not present, light rays do not escape and are continuously mixed up in a random fashion. The photonics sea generated is expected to follows a classical random walk with no dilution, showing a Rayleigh intensity distribution characterized by waves with random phases distributed in the whole interval $[0, 2\pi]$. When light rays can escape in the channels, conversely, they deplete the dynamics inside the cavity by their path. Such path cancellation effect is expected to be stronger for larger channel width d, due to the higher number of rays that can get out from the resonator. The uniform distribution of phases observed in the closed cavity is the result of the sum of all the ray paths of the closed system. It is therefore natural to expect that the removal of a set of paths can induce a gap in the phase distribution of the field. The larger the channel width d, in this intuitive picture, the larger the inaccessible region in phase space and the larger the corresponding dilution of the random walk. The relationship between the phase gap $\delta\phi$ and the output waveguide width d, however, is far from trivial, and we assess it via massively parallel Finite-Difference Time-Domain (FDTD) simulations with our code NANOCPP [32]. In order to ensure a high accuracy, we employed a high resolution of 40 points per internal wavelength. In order to model a realistic case, we consider the propagation of a supercontinuum source with wavelengths in $\lambda \in [1.535\mu m, 1.565\mu m]$ (i.e., $30nm$ bandwidth centered at $\lambda_0 = 1.55\mu m$), launched at the input waveguide of the PhC cavity. By applying the Prony algorithm [33], we extracted the probability distribution of the electromagnetic field amplitude and phase,

calculating the size of the largest phase gap $\delta\phi$ (Fig. 2b) and the electromagnetic energy (Fig. 2c) for different output channel widths d. The latter is varied by removing an integer number of rows from the photonic crystal lattice. As seen in Fig. 2b, a variation of d creates a phase gap $\delta\phi$ with a nonlinear relationship. For $d \geq 3$, a small gap of $\approx \pi/10$ opens up, which slowly increases in size for larger d. In order to investigate the most favorable condition for the observation of these phenomena, we first calculate the average energy density $\eta =< \mathcal{E} >$:

$$\eta =< \mathcal{E} >= \int \mathcal{E}' P(\mathcal{E}') d\mathcal{E}', \tag{4}$$

with $P(\mathcal{E})$ the probability distribution of the electromagnetic energy density in the system. The average density η can be used to measure the largest deviation from the Rayleigh law, corresponding to the probability of observing a rare event, and therefore acts as an order parameter for the observation of rogue waves in the structure. Figure 2d reports the behavior of η versus waveguide spacing d, showing a maximum around $d = 7$. This dependence highlights the competition between a) a larger gap in phase space due to the increase of d (see Fig. 2b) and b) the reduction of the chaotic strength of the cavity resulting from the presence of larger output waveguides. This aspect is further illustrated by a set of classical billiard simulations (see SI).

Figure 3 summarizes our FDTD results in the optimal case $d = 7$, showing the spatial distribution of the electromagnetic energy density inside the cavity when an isolated rogue wave is formed in both space (Fig. 3a-c) and time (Fig. 3d-e). To further verify the rogue nature of the observed pattern, other than the anomalous deviation from the exponential shown in Fig. 2c-d, we also calculate the Significant Wave Height (SWH). The latter is defined as the average of the highest one-third of the waves nearby and represents a widely accepted parameter for the identification of rogue waves. Rogue waves are characterized by a maximum peak that is at least two times larger than the SWH [34]. This threshold criterion has been initially introduced in hydrodynamics, and is therefore formulated with reference to the wave amplitude. In order to comply as close as possible with its original formulation, we measure the SWH with reference to the electromagnetic wave amplitude, which is a parameter accessible from our FDTD simulations. The spatial hot spot displayed in Fig. 3 meets this criterion, as its energy density is 2.51 times higher in space and 2.20 times higher in time than its SWH. The subwavelength nature of the rogue wave is readily evaluated by applying Eq. (3) (Fig. 3c dashed line), showing a perfect agreement with

the result of FDTD (Fig. 3c solid line) and confirming a clear localization which is 25% smaller than the diffraction limit ($\lambda/2n = 230nm$, being n the effective index of the guided modes inside the cavity, which in 2D corresponds to the cavity refractive index). The time evolution of the rogue wave, exhibits a FWHM of approximatively 250 fs, which well matches Eq. (3) by using the full input pulse bandwidth $\delta\lambda = \lambda_0^2\delta\omega/2\pi c = 30nm$ (Fig. 3e). Quite remarkably, this means that such rogue waves are coherently accessing the spectral energy contained in the whole frequency bandwidth of the field. This also identify the maximum value in Fig. 2 as the maximum energy that we can extract for the given input bandwidth of $30nm$.

Imaging extreme events at the nanoscale

We now set out to observe nanoscale RWs on our chips. We begin by fabricating a series of silicon on insulator planar photonic crystal cavities with output couplers of different widths. The fabrication of optical resonators is realized by a silicon on insulator (SOI) substrate consisting of a 220 nm thick silicon layer on a 2 μm thick layer of SiO2. The patterns were written using ZEP resist with a modified LEO/RAITH electron-beam lithography system with 2 nm step size, then etched with a balanced blend of SF6 and CHF3 gases in a reactive ion etching step. After stripping off the residual resist, the sample was cleaved for end-fire coupling [35]. In our experiments, we launch 1550 nm, 150 fs light pulses into these resonators and image the electromagnetic field with an NSOM (see Methods for more details). In similar fashion with the FDTD analysis, we experimentally recorded the RW dynamics only after the light pulse has been bounced inside the cavity for a sufficiently long time, and when a photonic sea is generated. NSOM experiments measure both real $R_j(\mathbf{r})$ and imaginary $C_j(\mathbf{r})$ components of the electromagnetic field in the complex representation $E_j(\mathbf{r}) = R_j + iC_j$ $(j = x, y)$. The field intensity $\mathcal{I}$ obtained from NSOM experiments is expressed as follow:

$$\mathcal{I} = R_x^2 + R_y^2 + C_x^2 + C_y^2. \tag{5}$$

In a classical random walk condition, R_j and C_j are Normally distributed and the intensity probability generalizes the Rayleigh distribution to a chi-squared probability density with 4

degrees of freedom:

$$P(\mathcal{I}) = \frac{\mathcal{I}}{4\Gamma(4)} e^{-\frac{\mathcal{I}}{2}}, \tag{6}$$

being Γ the Gamma function. At large intensity, Eq. (6) is well described by Rayleigh law while at low $\mathcal{I}$ its shape is characterized by a pronounced peak. In order to compare NSOM experiments with FDTD data, we observe that Eq. (5) corresponds to the time average of the electromagnetic field in the real space, i.e., $\mathcal{I} = \bar{\mathcal{E}}$, with $\bar{\mathcal{E}}$ denoting a time average of $\mathcal{E}$ over one optical cycle. Figures 4a-c summarize the statistical analysis of light dynamics inside the optical resonator, providing a quantitative comparison between theory and experimental NSOM results. Figure 4a consider the case for $d = 1$, comparing the classical random walk condition from NSOM measurements (triangle markers) and the analytical estimates of Eq. 6 (dashed line). Consider the rare nature of the phenomenon under study, the agreement between theory and experiments is quite remarkable. Figure 4b then compares the experimental retrieved energy distribution in the optimal case $d = 7$ for the observation of RWs (circle markers), with the theoretical predictions of FDTD simulations (triangle markers) and our random wave model described by Eq. 1 (diamond markers). Even in this case the matching between theory and experiments is extremely high. Figures 4a-b also illustrate the high level of control offered by our integrated chips in the generation of these events.

Figure 4c shows a photo sequence of the spatial distribution of the electromagnetic energy when an ultrafast subwavelength rogue wave is formed by spontaneous waves synchronizations. The intensity distributions along x (Fig. 4d) and in time (Fig. 4d) well match with our FDTD predictions (Fig. 3c-e). The agreement between simulation and experiment is further supported by the significant wave height ratio, which is measured to be 2.41 in space and 2.1 in time. As in our FDTD simulations, we measured the SWH with reference to the field amplitude, which is accessible in each NSOM experiment. When illustrating our experimental results (4c), conversely, we normalized the field energy by the significant wave height calculated from the field intensity, which we indicated with SWHI in order to distinguish it from the SWH calculated from the field amplitude. The SWHI of the rogue wave is ≈ 6 and corresponds roughly to two times the value 2.41 calculated from the field amplitude. Experimentally generated rogue waves exhibit a subwavelength spatial FWHM of $206nm$, which is 25% smaller than the diffraction limit $\lambda/2n = 287nm$ (with $n = 2.7$ the three dimensional effective index of the guided modes inside the cavity). The temporal

FWHM extension of the rogue wave, conversely, is 163 fs and corresponds to a bandwidth of $\delta\lambda = 49nm$, which matches the full electromagnetic field bandwidth ($\approx 50nm$). As a further proof of the repeatability of our results, we added a second NSOM image of the formation of an ultrafast subwavelength rogure wave, appearing at a different spatio-temporal position, in the supplementary information of the manuscript.

DISCUSSION AND CONCLUSION

We have proposed and demonstrated a simple integrated platform that generates ultrafast rare events, which exploit the spectral energy of the full frequency bandwidth of an incoherent field to buildup nanostructures of light of giant intensity. Using a planar photonic crystal cavity platform, we then demonstrated the generation of 165fs long, 206nm wide rogue waves at the wavelength of $\lambda_0 = 1.55\mu m$. Our analytical model, FDTD simulations and experimental observations agree extremely well, showing that the statistics of these ultrashort subwavelength coherent structures can be generated on demand, including their spatio-temporal shape.

Our chaotic resonators open up new possibilities, both in fundamental and applied science. Compared to nanoplasmonic structures, they also achieve subwavelength localization, but without using tapered metal nanostructures, specific nanoantenna designs or lossy materials. In addition, they do not require the use of coherent fields, and the appearance of localized energy spots is not limited in the near field. In our experiments, we observe rogue waves whose mutual distance is $\approx 50\mu m$, which corresponds ≈ 120 wavelengths in Si and is far beyond the near field distance of nanoplasmonic hot energy spots. Compared to other methods for generating sub-diffraction limited light using randomness, no sophisticated spatial light modulator system is required. In the above mentioned cases (plasmonic structures and random systems), evanescent contributions beyond the diffraction cutoff are generated. The use of rare events provides an alternative approach, where diffraction limited components are exploited in very simple dielectrics.

We can identify many applications that may benefit from such an extreme light-matter interaction, where their appearance is not constrained to any specific position but conversely requires a large intensity and a given distribution. These range from extremely sensitive spectrometers based on speckles [36], to new sensing apparatus based on random light patterns

randomly displaced in two dimensions [37], to low-threshold lasers sustained by randomly localized electromagnetic modes [38], and new energy harvesting devices relying on chaotic light motion [32].

An important aspect concerns the suppression of detrimental or destructive manifestations of rogue waves, which other than the open sea [39] appear to be relevant also in high speed data communication [40]. Our results shown in Fig. 2d open an interesting question wether or not RW can be completely eliminated by either increasing chaos or the system losses, which can stimulate interesting work in both nonlinear optics and hydrodynamics. The interplay between nonlinearity and spontaneous waves synchronization is also an issue of of fundamental interest. A thorough investigation on this topic is clearly beyond the scope of this work, however, some interesting points can be highlighted. In the present work we exploit the mechanism of wave chaos to randomize the dynamics of electromagnetic waves in phase-controlled conditions, which are settled by specific waveguide channels. Extremely localized rare events then emerge from a totally incoherent field, where the phases are fully delocalized between 0 and 2π. This opens up a new interesting panorama if compared to nonlinear dynamics, where rogue waves has predicted to appear only if the incoherence of the system is small enough [24]. Another very intriguing point is related to what can happen if such random ensemble evolves into a cavity with a fully nonlinear response. The nontrivial interplay between spontaneous synchronizations and classical Kerr nonlinearities [23] can furnish new important results in the study of rare events in physics.

Methods

Near-field scanning optical microscopy. — To image the light-field distributions inside the chaotic resonators we use a home-built NSOM, whose operation is described in detail in [29, 41], and therefore we here limit to present the main results. Briefly, an aperture probe that consists of an aluminum-coated tapered SiO2 fiber with a 100-300 nm sized aperture, is placed at a distance of 20 nm of the surface, within the evanescent tail of the electromagnetic field inside the cavity. This aperture converts a small fraction of the near field to far-field radiation that is transported through the fiber to a detector, and by raster scanning the probe across the cavity we can construct a two dimensional map of the electromagnetic field inside cavity. To detect this inherently weak signal we use a heterodyne detection scheme

where the microscope is placed in one branch of a Mach-Zehnder interferometer and interfere the signal from the probe with a reference pulse. This approach both amplifies our signal, and by placing and scanning a delay line in one of the branches, it also allows us to obtain temporal information.

Acknowledgments

For the computer time, we used the resources of the KAUST Supercomputing Laboratory and the Redragon cluster of the Primalight group. This work is part of the research program of Kaust "Optics and plasmonics for efficient energy harvesting" and the Foundation for Fundamental Research on Matter (FOM), which is part of the Netherlands Organisation for Scientific Research (NWO). This work is supported by Kaust (Award No. CRG-1-2012-FRA-005), by NanoNextNL of the Dutch ministry EL&I and 130 partners and by the EU FET project "SPANGL4Q".

Authors contributions

A. F. initiated the work and develop the theoretical model for the controlled formation of rogue waves. C. Liu performed FDTD simulations. R. E. C. W., N. R., and L. K. realized NSOM measurements. A. D. F fabricated samples used in experiments. All authors contributed equally in the analysis and interpretation of experimental results. All authors contributed to write the manuscript.

---

[1] Oulton, R. F. *et al.* Plasmon lasers at deep subwavelength scale. *Nature* **461**, 629–632 (2009).

[2] Chen, J. *et al.* Optical nano-imaging of gate-tunable graphene plasmons. *Nature* (2012).

[3] Gramotnev, D. K. & Bozhevolnyi, S. I. Plasmonics beyond the diffraction limit. *Nature Photonics* **4**, 83–91 (2010).

[4] Lerman, G. M., Yanai, A. & Levy, U. Demonstration of nanofocusing by the use of plasmonic lens illuminated with radially polarized light. *Nano letters* **9**, 2139–2143 (2009).

[5] Zhang, X. & Liu, Z. Superlenses to overcome the diffraction limit. *Nature Materials* 435–441 (2008).

[6] Schuller, J. A. *et al.* Plasmonics for extreme light concentration and manipulation. *Nature Materials* 192–204 (2010).

[7] Polman, A. & Atwater, H. A. Photonic design principles for ultrahigh-efficiency photovoltaics. *Nature Materials* 174–177 (2012).

[8] Rogers, E. T. F. *et al.* A super-oscillatory lens optical microscope for subwavelength imaging. *Nat. Material* **11**, 432–435 (2012).

[9] Kao, T. S., Rogers, E. T. F., Ou, J. Y. & Zheludev, N. I. Digitally addressable focusing of light into a subwavelength hot spot. *Nano Letters* **12**, 2728–2731 (2012).

[10] Choi, Y. *et al.* Overcoming the diffraction limit using multiple light scattering in a highly disordered medium. *Phys. Rev. Lett.* **107**, 023902 (2011).

[11] Vellekoop, I., Lagendijk, A. & Mosk, A. Exploiting disorder for perfect focusing. *Nature Photonics* **4**, 320–322 (2010).

[12] Katz, O., Small, E., Bromberg, Y. & Silberberg, Y. Focusing and compression of ultrashort pulses through scattering media. *Nature photonics* **5**, 372–377 (2011).

[13] Krauss, G. *et al.* Synthesis of a single cycle of light with compact erbium-doped fibre technology. *Nature Photonics* 33–36 (2010).

[14] Oktem, B., Ülgüdür, C. & Ilday, F. O. Soliton-similariton fibre laser. *Nature Photonics* 307–311 (2010).

[15] Onorato, M., Osborne, A. R., Serio, M. & Bertone, S. Freak waves in random oceanic sea states. *Phys. Rev. Lett.* **86**, 5831–5834 (2001).

[16] Ganshin, A. N., Efimov, V. B., Kolmakov, G. V., Mezhov-Deglin, L. P. & McClintock, P. V. E. Observation of an inverse energy cascade in developed acoustic turbulence in superfluid helium. *Phys. Rev. Lett.* **101**, 065303 (2008).

[17] Höhmann, R., Kuhl, U., Stöckmann, H.-J., Kaplan, L. & Heller, E. J. Freak waves in the linear regime: A microwave study. *Phys. Rev. Lett.* **104**, 093901 (2010).

[18] Solli, D. R., Ropers, C., Koonath, P. & Jalali, B. Optical rogue waves. *Nature* **450**, 1054–1057 (2007).

[19] Dudley, J. M., Genty, G. & Eggleton, B. J. Harnessing and control of optical rogue waves in supercontinuum generation. *Opt. Express* **16**, 3644–3651 (2008).

[20] Kasparian, J., Béjot, P., Wolf, J.-P. & Dudley, J. M. Optical rogue wave statistics in laser filamentation. *Opt. Express* **17**, 12070–12075 (2009).

[21] Bosco, A. K. D., Wolfersberger, D. & Sciamanna, M. Extreme events in time-delayed nonlinear optics. *Opt. Lett.* **38**, 703–705 (2013).

[22] Marsal, N., Caullet, V., Wolfersberger, D. & Sciamanna, M. Spatial rogue waves in a photorefractive pattern-forming system. *Optics Letters* (2014).

[23] Picozzi, A. *et al.* Optical wave turbulence: Towards a unified nonequilibrium thermodynamic formulation of statistical nonlinear optics. *Physics Reports* **504**, 1–132 (2014).

[24] Hammani, K., Kibler, B., Finot, C. & Picozzi, A. Emergence of rogue waves from optical turbulence. *Phys. Lett. A* **374**, 3585–3589 (2010).

[25] Onorato, M., Residori, S., Bortolozzo, U., Montina, A. & Arecchi, F. Rogue waves and their generating mechanisms in different physical contexts. *Physics Reports* **528**, 47 – 89 (2013).

[26] Bonatto, C. *et al.* Deterministic optical rogue waves. *Phys. Rev. Lett.* **107**, 053901 (2011).

[27] Baronio, F., Degasperis, A., Conforti, M. & Wabnitz, S. Solutions of the vector nonlinear schrödinger equations: Evidence for deterministic rogue waves. *Phys. Rev. Lett.* **109**, 044102 (2012).

[28] Stöckmann, H. J. *Quantum Chaos: An Introduction* (Cambridge Press, Cambridge, 2007).

[29] Sandtke, M. *et al.* Novel instrument for surface plasmon polariton tracking in space and time. *Rev. Sc. Instr.* **79**, 013704–(10) (2008).

[30] Rudnick, J. & Gaspari, G. *Elements of the Random Walk: An introduction for Advanced Students and Researchers* (Cambridge University Press, New York, 2010).

[31] Berry, M. V. A note on superoscillations associated with bessel beams. *Journal of Optics* **15**, 044006–(4) (2013).

[32] Liu, C. *et al.* Enhanced energy storage in chaotic optical resonators. *Nature Photonics* **7**, 473–478 (2013).

[33] Tijhuis, A. G. *Electromagnetic Inverse Profiling, Theory and Numerical Implementation* (VNU Science Press, 1987).

[34] Dysthe, K., Krogstad, H. E. & Mller, P. Oceanic rogue waves. *Annual Review of Fluid Mechanics* **40**, 287–310 (2008).

[35] Falco, A. D., Krauss, T. F. & Fratalocchi, A. Lifetime statistics of quantum chaos studied by a multiscale analysis. *Appl. Phys. Lett.* **100**, 184101 (2012).

[36] Redding, B., Liew, S. F., Sarma, R. & Cao, H. Compact spectrometer based on a disordered photonic chip. *Nature Photonics* **7**, 746–751 (2013).

[37] Cohen, S. D., de S. Cavalcante, H. L. D. & Gauthier, D. J. Subwavelength position sensing using nonlinear feedback and wave chaos. *Phys. Rev. Lett.* **107**, 254103 (2011).

[38] Conti, C., Leonetti, M., Fratalocchi, A., Angelani, L. & Ruocco, G. Condensation in disordered lasers: Theory, simulations, and experiments. *Phys. Rev. Lett.* **101**, 143901–(4) (2008).

[39] Cahill, B. G. & Lewis, A. W. Resource variability and extreme wave conditions at the atlantic marine energy test site (2011). 4th International Conference on Ocean Energy (ICOE), 17-19 October, Dublin.

[40] Vergeles, S. & Turitsyn, S. K. Optical rogue waves in telecommunication data streams. *Phys. Rev. A* **83**, 061801 (2011).

[41] Rotenberg, N. & Kuipers, L. Mapping nanoscale light fields. *Nat. Photon.* **8**, 919–926 (2014).

FIGURE LEGENDS

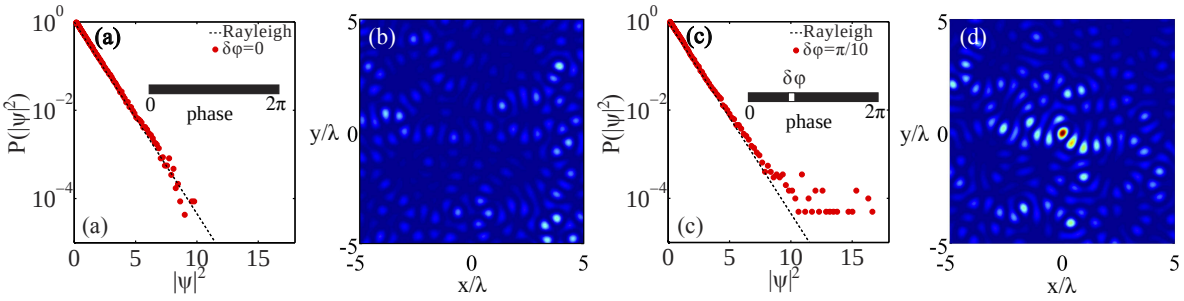

FIG. 1. Classical and diluted random walks of photons: intensity probability density (a,c) and spatial wave pattern at $t = 0$ (b,d) generated by and ensemble of 2000 random waves with uniformly (a-b) and diluted (c-d) phase distribution. Dilution is realized by inserting a small gap $\delta\phi = \pi/10$ of inaccessible values in the probability distribution of ϕ (c, inset). By comparing (b) and (d), we observe the spontaneous formation of a rogue wave in the chaotic light pattern. In all simulations, we consider a randomly displaced wavevector $\mathbf{k}$ in the plane and uniformly distributed amplitudes $a \in [0, 1]$ and frequencies $\omega \in [1, 2]$.

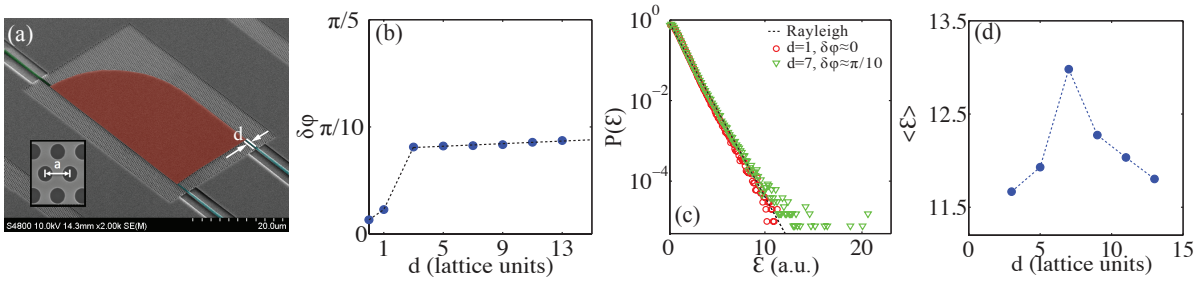

FIG. 2. Photonic crystal resonator: design and FDTD simulations. (a) SEM image of the structure with the resonator area highlighted in false color; (b) largest gap $\delta\phi$ in the phase probability density versus waveguide spacing d; (c) electromagnetic energy density $\mathcal{E}$ probability distribution for $d = 1$ (circle markers), $d = 7$ (triangle markers) and a classical random walk process (dashed line); (d) order parameter $\eta =< \mathcal{E} >$ versus d.

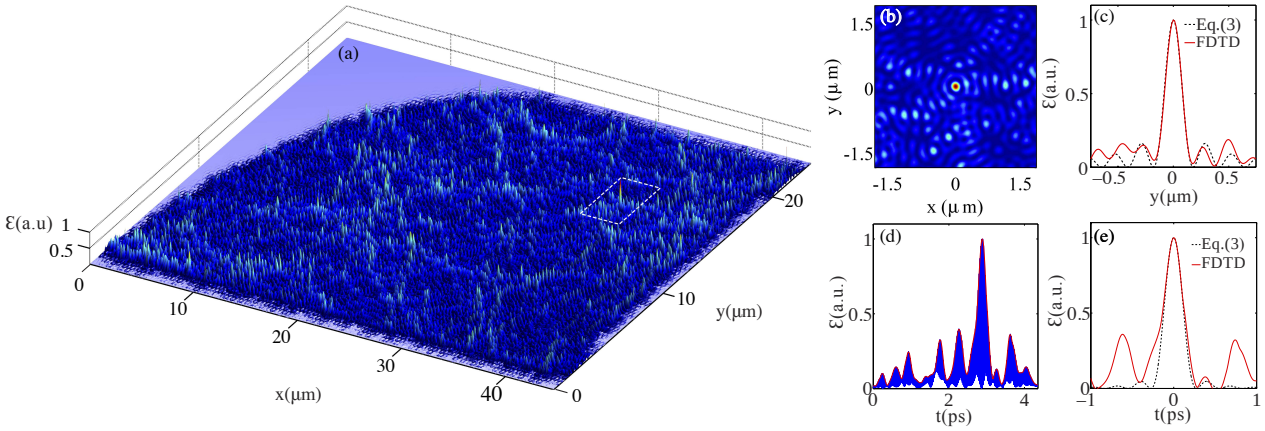

FIG. 3. FDTD analysis of ultrafast subwavelength light localization: (a) electromagnetic energy distribution in the cavity in the presence of an extremely localized rogue wave and (b) zoomed detail on the RW energy peak; (c) section of the energy distribution along y (solid line) versus theoretical prediction based on our random wave model (dashed line); (d) temporal dynamics of the RW spatial energy peak. Panel (e) shows a detailed dynamics of panel (d) with the corresponding theoretical prediction (dashed line). In panel b-c and e, we centered the axis origin with respect to the intensity maximum of the rogue wave.

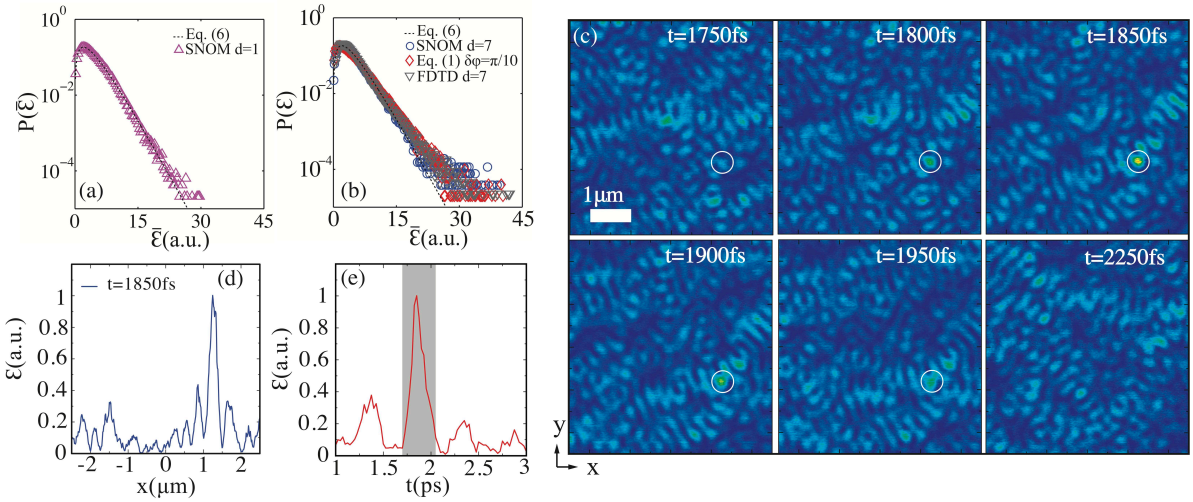

FIG. 4. Summary of NSOM experimental results and comparison with theory. Panel a compares the time averaged energy probability density $P(\bar{\mathcal{E}})$ retrieved from NSOM experiments for $d = 1$ (triangle markers). Panel b compares FDTD results (triangle markers) and NSOM experiments for the case of $d = 7$ (circle markers), with Eq. (1) for $\delta\phi = \pi/10$ (diamond markers). In both panels, we also show the probability law dependence of the classical random walk (dashed line) for reference. Panels c displays the time evolution of the electromagnetic energy density when a nanoscale rogue wave settles in, with panel d showing a section of the energy distribution along x when the rogue wave exhibits the maximum intensity. Panel e, finally, reports the temporal dynamics of the rogue wave energy peak. In panel c, the color bar on the left indicates the values of the electromagnetic energy density, which was normalized respect to the significant wave height of the field intensity (SWHI).